Title

Large-scale plant light-use efficiency inferred from the seasonal cycle of atmospheric CO2

Journal

Global Change Biology, 10(8)

ISSN

1354-1013

Authors

Still, Christopher J
Randerson, J T
Fung, I Y

Publication Date

2004-08-01

Peer reviewed

Global Change Biology (2004) **10,** 1240–1252, doi: 10.1111/j.1365-2486.2004.00802.x

Large-scale plant light-use efficiency inferred from the seasonal cycle of atmospheric CO_2

CHRISTOPHER J. STILL*, JAMES T. RANDERSON† and INEZ Y. FUNG*
*Berkeley Atmospheric Sciences Center, 307 McCone Hall, University of California, Berkeley, CA 94720-4767, USA,
†Earth System Science Department, 3212 Croul Hall, University of California, Irvine, CA 92697-3100, USA

Abstract

We combined atmospheric CO_2 measurements, satellite observations, and an atmospheric transport model in an inverse modeling framework to infer a key property of vegetation physiology, the light-use efficiency (LUE) of net primary production, for large geographic regions. We find the highest LUE in boreal regions and in the northern hemisphere tropics. Within boreal zones, Eurasian LUE is higher than North American LUE and has a distinctly different seasonal profile. This longitudinal asymmetry is consistent with ecological differences expected from the much greater cover of deciduous vegetation in boreal Eurasia caused by the vast Siberian forests of the deciduous conifer, Larch. Inferred LUE of the northern hemisphere tropics is also high and displays a seasonal profile consistent with variations of both cloud cover and C_4 vegetation activity.

Keywords: C_4 photosynthesis, CO_2 seasonal cycle, diffuse radiation, global ecology, inverse modeling, Larch

Received 10 February 2003; revised version received 8 December 2003 and accepted 12 January 2004

Introduction

Measurements of atmospheric CO_2 concentration at remote monitoring stations constrain large-scale terrestrial carbon fluxes. In combination with atmospheric transport models and inversion modeling, these concentration data suggest a large northern hemisphere terrestrial carbon sink during most of the last decade (Enting *et al*., 1995; Fan *et al*., 1998; Rayner *et al*., 1999; Bousquet *et al*., 2000; Pacala *et al*., 2001; Rayner, 2001; Gurney *et al*., 2002). The spatial distribution of this sink has been the subject of intense scrutiny, especially the partitioning of net carbon exchanges between Eurasia and North America. Most inversion results suggest asymmetries in the magnitude of carbon storage between these continental regions. For example, one result (Fan *et al*., 1998) places most of the northern hemisphere terrestrial carbon sink in North America, while recent studies suggest a more even balance, albeit with the majority located in Eurasia (Rayner *et al*., 1999; Bousquet *et al*., 2000; Pacala *et al*., 2001; Gurney *et al*., 2002).

Correspondence: Christopher Still, Geography Department, 3611 Ellison Hall, University of California, Santa Barbara, Santa Barbara, CA 93106, USA, tel. 805-893-5501, fax 805-893-2578, e-mail: cstill@geog.ucsb.edu

In addition to using the inversion approach to solve for sources and sinks of carbon, it is also possible to solve for key parameters that regulate ecosystem function. In this study, we present an inversion calculation of the light-use efficiency (LUE) for large land regions on a seasonal basis. We use the inferred LUE patterns to test ecological theory underlying biosphere models and to improve our understanding of ecosystem processes and the carbon cycle across multiple scales. Specifically, we evaluate our results against broad-scale vegetation distributions and the composition of downwelling solar radiation, as well as carbon storage patterns from recent inversion results.

One of the simplest approaches for predicting net primary production using such biosphere models is the 'light-use' or 'production' efficiency model (Monteith, 1977) that has been adapted for global simulations (Potter *et al*., 1993; Ruimy *et al*., 1994, 1999; Field *et al*., 1998). In this 'bottom-up' approach, net primary production (NPP), or the difference between gross photosynthesis and autotrophic respiration, is assumed to be proportional to absorbed photosynthetically active radiation, or APAR, with the proportionality coefficient being the LUE term:

$$\mathrm{NPP}(x,t) = \mathrm{LUE}(x,t) * \mathrm{APAR}(x,t).$$

Spatial and temporal variations in APAR are prescribed from surface irradiance and the fraction of incident photosynthetically active radiation (fPAR) absorbed by vegetation, derived from satellite observations (Potter *et al*., 1993; Ruimy *et al*., 1994; Field *et al*., 1998; Ruimy *et al*., 1999).

The LUE term represents a conversion efficiency, or the ratio of carbon biomass produced for each unit of absorbed light. In natural ecosystems, LUE is determined by many biological and biophysical factors, principally, maximum photosynthetic rates under light-saturated conditions, fraction of photosynthesis consumed by autotrophic respiration, quantum yield of photosynthesis, photosynthetic pathway (C_3 vs. C_4), and climate (Monteith, 1977; Potter *et al*., 1993; Running & Hunt, 1993; Ruimy *et al*., 1994; Goetz & Prince, 1998; Field *et al*., 1998; Ruimy *et al*., 1999; Choudhury, 2001). Additionally, recent experimental (Gu *et al*., 2002) and theoretical work (Roderick *et al*., 2001) has shown that canopy-scale LUE is positively related to the diffuse fraction of irradiance, and thus, cloud conditions. Estimates of LUE are not well constrained and provide a large source of error in model estimates of global NPP (Field *et al*., 1998; Ruimy *et al*., 1999). This disagreement among models arises from different philosophies on the environmental and biological controls of LUE and the methods adopted to estimate this parameter. In one approach, LUE departs from a theoretical universal optimum due to climatic variations (Potter *et al*., 1993), whereas a contrasting approach assigns LUE values by vegetation functional types (Ruimy *et al*., 1994). However, the two approaches are not mutually exclusive.

Although very different in concept and methodology, the inverse, or 'top-down', method and the forward, or 'bottom-up', method are complementary approaches to estimating CO_2 exchange between the atmosphere and terrestrial biosphere (Dargaville *et al*., 2002). The standard inverse method takes advantage of atmospheric CO_2 observations that provide an integral constraint on net surface carbon fluxes, but little additional information about the underlying mechanisms. In contrast, the forward approach incorporates process-level understanding to predict the net carbon flux, but suffers from uncertainties in estimating model parameters and scaling carbon fluxes from study sites to larger scales. Recently, several studies (Knorr & Heimann, 1995; Kaminski *et al*., 2002; Randerson *et al*., 2002) have attempted to relate the approaches by constraining terrestrial biosphere model parameters using CO_2 observations and atmospheric transport models. Knorr & Heimann (1995) explored atmospheric CO_2 constraints on a simple terrestrial biosphere model by tuning a single global LUE and temperature sensitivity of heterotrophic respiration (Q_{10}) to best match the CO_2 observations. Randerson *et al*. (2002) used CO_2 concentration data to obtain a single optimal combination of LUE and Q_{10} for northern land areas, and then used the optimized ^{12}C exchanges and atmospheric carbon isotope data to infer terrestrial ^{13}C discrimination in these regions. Kaminski *et al*. (2002), extending a concept proposed earlier by Rayner (2001), pioneered the use of data assimilation techniques in terrestrial biosphere models. They directly assimilated atmospheric CO_2 concentration data into a biosphere model to infer an optimal value of LUE and Q_{10} for each of 12 biomes. Our study builds on these approaches to extend our understanding of large-scale ecological function and examine underlying physiological controls on carbon exchange processes. We incorporate, *a priori*, satellite-derived fields of APAR, thus augmenting the data input into the underdetermined inversion.

Materials and methods

The land surface was divided into eight large geographic areas (basis regions). After accounting for ocean and fossil fuel influences, the atmospheric CO_2 seasonal cycle results from the balance between NPP and heterotrophic respiration (HR), and so the inferred LUE for these regions must be sensitive not only to the APAR fields, but also to the representation of HR. We, conducted four inversion experiments to test the sensitivity of our results to model inputs. We tested two different fields of APAR, HR, and air–sea gas exchange. In each inversion experiment, we calculated a flux-weighted, growing-season mean LUE for each land basis region. The growing season was defined as the period when the average monthly mean APAR exceeded $25\,MJ\,m^{-2}$. Monthly errors were added in quadrature to estimate the growing-season mean LUE standard error for each basis region in each experiment. The flux-weighted, growing-season mean LUE values and associated errors from each inversion experiment were then used to calculate the overall mean LUE and error for each basis region. The CO_2 concentration data, inversion methodology, and model inputs of HR, APAR and air–sea gas exchange are described in the following sections.

CO_2 seasonal cycle data

The CO_2 seasonal cycle data used in the inversion were taken from the GLOBALVIEW-CO_2 product (GLOBALVIEW-CO_2, 2001). We included only those stations located in the remote marine boundary layer or at continental edges; ocean cruise data were not used. The thirty stations used in our study are listed in Table 1. The GLOBALVIEW-CO_2 product provides mean seasonal

Table 1 The NOAA-CMDL monitoring stations used in this study

Station name and description	Latitude and longitude (°)	
Alert Island, Nunavut, Canada	82.45	−62.52
Ascension Island, UK	−7.92	−14.42
St. David's Head, Bermuda, UK	32.37	−64.65
Tudor Hill, Bermuda, UK	32.27	−64.88
Barrow, Alaska, USA	71.32	−156.60
Cold Bay, Alaska, USA	55.20	−162.72
Cape Grim, Tasmania, Australia	−40.68	144.68
Crozet Island, France	−46.45	51.85
Easter Island, Chile	−27.15	−109.45
Guam, Mariana Islands, USA	13.43	144.78
Dwejra Point, Gozo, Malta	36.05	14.18
Halley Bay, Antarctica, UK	−75.67	−25.50
Heimaey, Vestmannaeyjar, Iceland	63.25	−20.15
Tenerife, Canary Islands, Spain	28.30	−16.48
Key Biscayne, Florida, USA.	25.67	−80.20
Cape Kumukahi, Hawaii, U.S.A.	19.52	−154.82
Mould Bay, Nunavut, Canada	76.25	−119.35
Mace Head, County Galway, Ireland	53.33	−9.90
Sand Island, Midway, USA	28.22	−177.37
Mauna Loa, Hawaii, USA	19.53	−155.58
Palmer Station, Antarctica, USA	−64.92	−64.00
Ragged Point, Barbados	13.17	−59.43
Mahe Island, Seychelles	−4.67	55.17
Shemya Island, Alaska, USA	52.72	174.10
Tutuila, American Samoa, USA	−14.25	−170.57
South Pole, Antarctica, USA	−89.98	−24.80
Ocean Station 'M', Norway	66.00	2.00
Syowa Station, Antarctica, Japan	−69.00	39.58
Sede Boker, Negev Desert, Israel	31.13	34.88
Ny-Alesund, Svalbard (Spitsbergen), Norway/Sweden	78.90	11.88

Station names and locations are given, along with coordinate data.

cycles for each station (12 values with associated standard deviations (SDs) for each) as calculated from a detrended smooth fit to the observations. We used the seasonal cycle data from stations in the NOAA Climate Monitoring and Diagnostics Laboratory (CMDL) network only. The number of records used to calculate mean seasonal cycles and SDs varied from station to station, but it was typically greater than five. The temporal coverage of the observations used to construct the GLOBALVIEW mean seasonal cycle product thus usually spanned the decade of the 1990s and in many cases part or most of the 1980s.

Inversion methodology

We used the Bayesian synthesis inversion formalism (Enting *et al*., 1995; Rayner *et al*., 1999; Bousquet *et al*., 2000; Gurney *et al*., 2000, 2002; Pacala *et al*., 2001) to infer the seasonal cycle of terrestrial light-use efficiency. In this approach, forward runs of an atmospheric transport model (Fung *et al*., 1991) are conducted to quantify the sensitivity of atmospheric CO_2 concentrations to surface fluxes. We used the same Goddard Institute for Space Studies (GISS) atmospheric transport model runs from an earlier study (Randerson *et al*., 2002). The land and ocean surface were divided into 16 geographical regions (eight basis regions each for ocean and land), and a 1 Pg pulse of carbon was emitted from each region every month into the transport model. The 1 Pg C pulse was distributed evenly in time over the month.

The land pulses within each basis region were released with the spatial distribution of mean annual NPP from the CASA model (Potter *et al*., 1993), consistent with the methodology of the Transcom experiment (Gurney *et al*., 2000). In other words, we used pulse functions whose spatial distribution is weighted by the spatial distribution of mean annual NPP. For the ocean basis regions, the 1 Pg C pulse was released with a uniform spatial distribution each month.

In the Bayesian approach, *a priori* estimates of the source fluxes with associated uncertainty are introduced, in this case, it is the prior guesses of LUE. We used uniform values of $0.45\,gC\,MJ^{-1}$ APAR for all regions and months, and an associated uncertainty of 50%. The prior guess on LUE is an intermediate value among the range of values predicted by process models, as summarized by Ruimy *et al*. (1999). The prior error was fairly large, ensuring that the inferred LUE estimates were determined primarily by observations. Further details on inversion methodology, including the cost function formulation, Bayesian estimation, and the least-squares minimization solution, are presented elsewhere (Enting *et al*., 1995; Rayner *et al*., 1999; Bousquet *et al*., 2000; Peylin *et al*., 2000; Pacala *et al*., 2001; Gurney *et al*., 2002).

We were interested in seasonal variations of LUE for each basis region. In the inversion taxonomy, such a seasonal approach is referred to as a 'cyclostationary' inversion, which assumes that both surface fluxes and atmospheric transport do not vary from year to year (Peylin *et al*., 2000). In this inversion, the optimal combination of monthly LUE values for each basis region was determined. Following previous works (Bousquet *et al*., 2000; Peylin *et al*., 2000), we stabilized the inversion by including conservative limitations on month-to-month differences in the inferred LUE for each region (no greater than $0.3\,gC\,MJ^{-1}$ APAR difference from month to month with an uncertainty of $0.1\,gC\,MJ^{-1}$ APAR). In practice, this is necessary

primarily for the southern hemisphere basis region (#8) since its fluxes impact the atmospheric seasonal cycle much less than northern hemisphere regions, and the inversion is free to infer unrealistically large month-to-month LUE fluctuations in this region given the large uncertainty we have applied to the Bayesian prior LUE estimates (cf. Peylin *et al.*, 2000). Including this month-to-month constraint only slightly affects the inferred temperate and high-latitude LUE values, as well as those for the northern hemisphere tropical basis region (#7).

Because carbon exchanges influencing the seasonal cycle of atmospheric CO_2 include oceanic and fossil fuel fluxes, these must be removed, or 'presubtracted,' before aspects of the terrestrial carbon cycle can be retrieved from the atmospheric record. For ocean exchanges from each region and month, we estimated the total net flux as a function of the partial pressure of CO_2 in surface seawater (Takahashi *et al.*, 1997), a gas transfer coefficient–wind speed relationship (Tans *et al.*, 1990), and a climatological monthly mean wind field (Esbensen & Kushnir, 1981). The concentration fields associated with oceanic exchanges were created using the flux fields and the oceanic pulse functions. Unlike the land pulse functions, the ocean pulse functions were released without any underlying spatial flux structure for each region (Gurney *et al.*, 2000). For fossil fuel fluxes, we used decadal emission estimates for the period 1950–1990 (Andres *et al.*, 1996). These emissions were combined with modeled fossil fuel pulse functions to estimate monthly 3-D concentration fields for 41 years. The pulse functions were monthly, but we used only one basis region with the spatial distribution of the pulse release conforming to data from Andres *et al.* (1996). The final 10 years of concentration (1981–1990) were detrended with a smoothing spline (Randerson *et al.*, 2002) and the mean seasonal cycle from fossil fuel emissions at each station was extracted. This time period corresponds fairly well with the mean seasonal cycle GLOBALVIEW-CO_2 data for many of the stations used in this analysis.

The concentration fields from ocean and fossil fuel fluxes were presubtracted from the GLOBALVIEW-CO_2 mean seasonal cycle observations at each station prior to the inversion. (The contribution of oceanic and fossil fuel fluxes to seasonal cycle amplitudes at all stations was small, never larger than 1.5 ppm.) We assumed the remaining mean seasonal cycle at each station was determined solely by terrestrial net carbon exchanges. Because these exchanges are primarily the difference between NPP and HR, we specified HR in order to solve for the NPP of each region and month. HR concentration fields were created from HR flux fields and the transport model flux-to-concentration response matrix, and the inversion solved for optimal NPP concentration fields. Because APAR for each region and month was prescribed from satellite observations, this amounted to varying LUE values for each region and month to produce the NPP values most consistent with the atmospheric CO_2 observations. The HR and APAR fields are described in the next section.

Sensitivity analysis

We conducted four inversions to assess the sensitivity of inferred LUE to the model inputs (HR, APAR, and oceanic gas exchange – Table 2). Another useful sensitivity test would have been to use different atmospheric transport models. However, for this study we used only one transport model. The sensitivity to each input was assessed by comparison with the control inversion (#1). Inversion #2 differed from #1 in the HR field input. The magnitude and phasing of HR predicted by the two approaches directly impacts the inferred NPP required to match the seasonal cycle of CO_2 (and thus the inferred LUE). The first HR field is from simulations with the terrestrial carbon cycle model, CASA (Potter *et al.*, 1993). This model predicts NPP on a monthly basis and tracks carbon fluxes through multiple pools to predict heterotrophic respiration as a function of pool size, lignin content, soil moisture and texture, and temperature. The CASA HR field used here is from an updated version of the model that has a new allocation algorithm, as well as more realistic representations of tropical fluxes due to an updated soil moisture calculation (Van der Werf *et al.*, 2003). The total annual flux was scaled to equal the flux from the second HR approach ($46\,Pg\,C\,yr^{-1}$) so they could be compared. Even after this scaling, there were significant differences in the seasonal phasing and magnitude of HR between the approaches.

The other HR field (denoted RP95 – downloaded from http://cdiac.ornl.gov) is from the study of Raich & Potter (1995). In contrast to the CASA approach,

Table 2 The inversion scenarios conducted in this study

Inversion	HR flux	Ocean flux	APAR field
1	CASA	Tans	82–90 NDVI
2	RP95	Tans	82–90 NDVI
3	CASA	Tans	82–90 FASIR–NDVI
4	CASA	Wanninkhof	82–90 NDVI

Fields of heterotrophic respiration, APAR, and air–sea gas exchange were systematically varied to assess model sensitivity to these inputs. Inversion #1 was taken as the control inversion. HR, heterotrophic respiration; APAR, absorbed photosynthetically active radiation.

monthly soil respiration is calculated with a statistical formulation that captures environmental controls on soil respiration derived from dozens of empirical studies. This formulation contains terms for an exponential dependence of soil respiration on air temperature (a Q_{10} relationship) and a term for the effect of soil moisture on respiration (using precipitation as a surrogate for soil moisture). There is no dependence on soil pool size or plant inputs as with the CASA HR fields. The Q_{10} of this formulation is 1.49, and the total annual flux is 46.2 Pg C, assuming $\sim 60\%$ of soil respiration is derived from heterotrophs (e.g., Trumbore *et al*., 2002). There are very few data available to assign spatial and temporal variations to the heterotrophic fraction, so we used 60% uniformly for all regions and months. An updated version of the soil respiration model (Raich *et al*., 2002) predicts a higher Q_{10}. The updated model has a Q_{10} of 1.72.

Although the CASA and RP95 models are similar in the Q_{10} value each uses and in the global sums of HR, the approaches are in fact quite different. We chose these models, in part, to bracket the range of respiration modeling approaches. The RP95 field is generally more variable than the CASA field, partly because of the hyperbolic response of soil respiration to precipitation in the RP95 model. We conducted another inversion calculation (not one of the four sensitivity analyses reported here) with different Q_{10} values by employing both model A and model B from Raich & Potter (1995). Model A from RP95 has a Q_{10} value of 1.6 vs. 1.5 for model B (the latter was the model we used in our inversion sensitivity analysis). The inferred, growing-season mean LUE values change slightly between the runs, with higher values for Model A during the summer months. In general, as discussed previously by Lloyd & Farquhar (1994), Knorr & Heimann (1995), and Randerson *et al.* (2002), a higher Q_{10} value will produce higher summertime respiration fluxes. This would require higher summertime NPP and thus LUE values to match the CO_2 seasonal cycle.

Inversions #1 and #3 differed in the APAR inputs. For the first input, we derived 12 monthly APAR values for each basis region from mean values of the normalized difference vegetation index (NDVI) at 1×1 over the 1982–1990 period (Randerson *et al*., 1997) and mean monthly values of surface incident PAR from July 1983–June 1991 (Bishop & Rossow, 1991). NDVI was used to estimate the fraction of incoming PAR absorbed by vegetation (fPAR) using the formulation from Sellers *et al.* (1996). APAR was calculated from the product of fPAR and PAR. NDVI fields from the work of Los *et al.* (2000) were used to create the second APAR input. These fields, referred to as FASIR–NDVI, are based on a technique that employs several corrections before calculating NDVI (Sellers *et al*., 1996; Los *et al*., 2000). These corrections are necessary because reflectance data can become compromised by sensor degradation, viewing geometry, cloud cover, and volcanic aerosols (Los *et al*., 1994; Sellers *et al*., 1996; Los *et al*., 2000). These NDVI fields also cover the 1982–1990 period (Los *et al*., 2000). We calculated fPAR with the same formulation used for the first NDVI input field, and created a mean seasonal fPAR product by averaging values over the entire time period. For all land regions, the FASIR–NDVI fPAR product was higher than the NDVI fPAR product, though both displayed very similar mean seasonal patterns. As Los *et al.* (2000) note, interannual variations of the FASIR–NDVI data are much smaller than for uncorrected NDVI products over the same time period.

Inversions #1 and #4 differed in the air–sea gas exchange field used for presubtraction. The alternate air–sea gas exchange field was calculated using a quadratic relationship between gas transfer and wind speed (Wanninkhof, 1992).

Results and discussion

Overall, inferred LUE values were most sensitive to the choice of HR field. Because atmospheric concentration patterns are determined by the net land flux (after accounting for ocean and fossil fuel fluxes), which is the difference between HR and NPP, varying the timing and magnitude of HR directly impacts the NPP (and thus LUE) required to match the concentration data. In general, the RP95 HR field is more seasonal than the CASA HR field, and as a result the growing-season mean, flux-weighted LUE values are slightly higher with the RP95 HR field. Inferred LUE in high-temperate basis regions (3, 4) is slightly higher with RP95-HR, with little change in seasonality. Inferred LUE values in low temperate basis regions (5, 6) are essentially unchanged relative to the CASA HR case. We discuss sensitivity analysis results for the boreal and tropical basis regions later in the paper.

Varying the APAR fields (inversion #1 vs. #3) also impacted the inferred mean LUE, but with little impact on the seasonality of LUE in most regions. The FASIR–NDVI fields (#3) predict larger fPAR values in all regions with little change in the seasonality; the mean inferred LUE for all regions is correspondingly reduced. In general, underestimation of fPAR will lead to an increase in the inferred LUE.

Although the influence of oceanic gas exchange on the seasonal cycle of atmospheric CO_2 is generally small, using different parameterizations of the air–sea flux (inversion #1 versus #4) slightly impacts the

inferred terrestrial LUE in the high temperate and boreal land regions, with minimal impacts in other areas. Using the quadratic formulation (Wanninkhof, 1992) results in slightly lower LUE values in basis regions 2 and 3. The discrepancy results from different ocean fluxes in northern ocean basis regions predicted by this formulation.

The growing-season mean LUE values inferred for each land basis region are displayed in Table 3. These mean values were calculated by averaging the growing-season values from each inversion experiment given in Table 2. In general, the inferred LUE values are comparable with observations for vegetation functional groups (Ruimy *et al*., 1994; Running & Hunt, 1993; Gower *et al*., 1999). However, it is difficult and not always useful to compare modeling results such as ours with available ground-based measurements. One primary difficulty is the issue of scale, since the basis regions in our inversions cover millions of square kilometers, whereas the observations compiled by Gower *et al*. (1999) and Ruimy *et al*. (1994) are based on field studies covering areas usually much smaller than 10–100 km^2. Additionally, these field studies can focus on relatively pure ecotypes, whereas the basis regions in our study encompass numerous ecosystem types. Finally, there is a great variety in the metric of light utilization that is reported (Gower *et al*., 1999). Many of the data reported, especially from eddy flux studies, report values for the gross primary production LUE (GPP-LUE) (e.g., Turner *et al*., 2003) or canopy quantum yield (e.g., Hanan *et al*., 2003) on a daily basis, in contrast to many of the studies summarized in Ruimy *et al*. (1994) and Gower *et al*. (1999).

Our inversion results are also broadly consistent with the predictions of numerous biosphere models (Ruimy *et al*., 1999), other inversion studies (Knorr & Heimann, 1995; Randerson *et al*., 2002), and the assimilation modeling results of Kaminski *et al*. (2002), who used different methods, model inputs, and atmospheric transport model. Our results are particularly noteworthy in two regions where the inferred LUE values depart strongly from the prior LUE guesses: the boreal zones (north of 56°N) of North America and Eurasia (basis regions 1 and 2) and the northern tropics (all land 0–24°N – basis region 7).

Boreal regions

Inferred LUE in the boreal regions is much higher than other land regions, with the exception of region 7. Kaminski *et al*. (2002) also found higher LUE values at high latitudes. These results are higher than most field-based estimates from boreal regions (e.g., Lafont *et al*., 2002; Nichol *et al*., 2002), and likely result from the

Table 3 The land basis regions and the growing-season mean light-use efficiency (LUE) values (SE) inferred by the suite of inversions, in units of $gC\,MJ^{-1}$ APAR (absorbed photosynthetically active radiation) and mol $CO_2\,mol^{-1}$ APAR

Basis region number	Geographic description	Zonal coverage	Mean growing season LUE ($gC\,MJ^{-1}$ APAR)	Mean growing season LUE ($mol\,CO_2\,mol^{-1}$ APAR)	Reduction in inferred LUE error (%)	Mean growing season total cloud fraction
1	North American boreal	Ice-free land north of 56°N	0.67 (0.15)	0.013 (0.003)	33	0.69
2	Eurasian boreal	Ice-free land north of 56°N	0.79 (0.10)	0.016 (0.002)	56	0.68
3	N. American high temperate	40–56°N	0.50 (0.15)	0.010 (0.003)	33	0.67
4	Eurasian high temperate	40–56°N	0.40 (0.09)	0.008 (0.002)	60	0.63
5	N. American low temperate	24–40°N	0.44 (0.17)	0.009 (0.003)	24	0.56
6	Eurasian low temperate	24–40°N	0.44 (0.14)	0.009 (0.003)	38	0.61
7	Northern hemisphere tropics	0–24°N	0.61 (0.10)	0.012 (0.002)	56	0.63
8	Southern hemisphere	Ice-free land south of 0°	0.44 (0.07)	0.009 (0.001)	69	0.59

The growing season for each basis region was defined as the period when the monthly mean APAR exceeds 25 MJ PAR m^{-2}. Monthly errors were added in quadrature to estimate the growing-season mean SE for each basis region in each experiment. The mean LUE and uncertainty for each inversion-region combination were averaged across the four inversions. The reduction in LUE SE is relative to the prior error guess (SD) of 0.225 $gC\,MJ^{-1}$ APAR, so this error reduction is a slight overestimate (i.e., SE v. SD). Average total cloud fractions (Rossow *et al*., 1996) during the growing season were weighted by vegetation area in each region (DeFries *et al*., 1999).

stronger fluxes required to match seasonal cycles of CO_2 observed at these latitudes (Kaminski *et al*., 2002). Extensive and persistent cloudiness (Table 3) and presumed diffuse light fractions over boreal regions may also account in part for the high LUE values in these zones (Lafont *et al*., 2002; Randerson *et al*., 2002). However, there is no statistically significant correlation between our results and the cloudiness for either region.

Within boreal zones, the inferred LUE for Eurasia is consistently higher than North America (Table 3 and Fig. 1), although the growing-season mean values for these regions are not statistically separated at the 95% level. Indeed, only 1 month (June) has no overlap at the one-sigma SD level (Fig. 1). The LUE profile inferred for boreal Eurasia (open triangles in Fig. 1) is bell shaped with a maximum in July and August. In contrast, the LUE profile for boreal North America (filled circles) shows a sharp increase between June and July, stabilizing through the end of the growing season. The seasonal profiles for each region are consistent across all the inversions we conducted for our sensitivity analysis. It is unlikely the different profiles and seasonal averages are solely a function of climatic differences between the regions that would impact the LUE. We tested for the impact of climatic effects by separately calculating average LUE values for these regions using the CASA model (Potter *et al*., 1993), which predicts LUE by modifying an optimal value with temperature and moisture scalars. Both the seasonal profile and magnitude of LUE from the CASA approach were very similar for both boreal regions, suggesting that climatic effects alone cannot explain the inferred LUE differences. Additionally, the total cloud amount and presumed diffuse fraction of solar radiation are similar between regions throughout the year (Table 3), so these cannot account for the inferred LUE differences.

The different HR fields do not significantly impact the LUE inferred for boreal regions (1, 2). The seasonal shape of inferred LUE is very similar for these regions with differing HR fields (Fig. 2a); the RP95 HR field is slightly more seasonal than the CASA field, with larger peak summertime fluxes in basis region 1. This increases the corresponding summertime LUE required

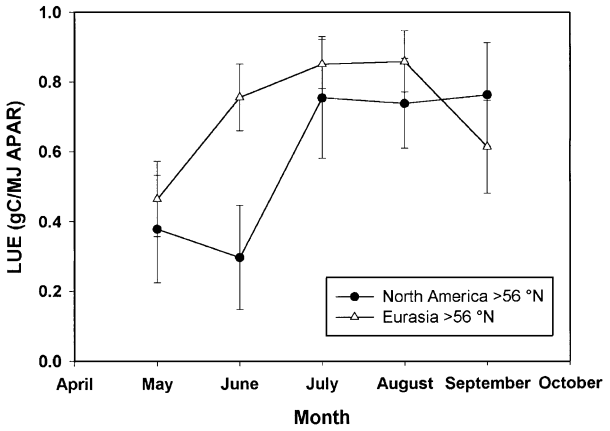

Fig. 1 Inferred growing-season LUE (gC MJ^{-1} APAR) with SD for land regions north of 56°N averaged across the four inversion experiments. North America is represented by filled circles, Eurasia is given by open triangles.

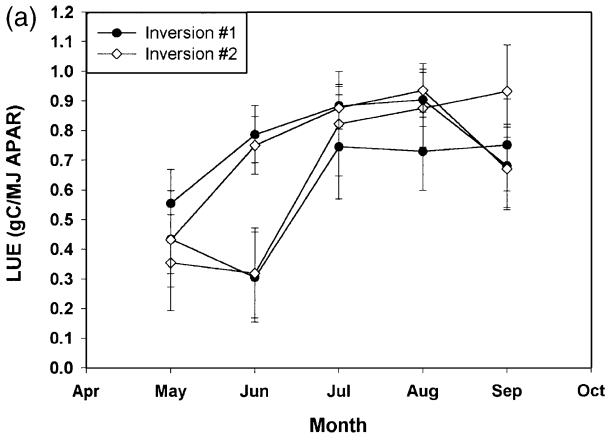

Fig. 2a (a) Inferred LUE (gC MJ^{-1} APAR) for boreal regions (1,2) for the base inversion (#1) and the scenario with alternate HR (RP95) field (inversion #2). Inversion #1 is represented by filled circles for both basis regions, and inversion #2 is given by open diamonds for both basis regions. (b) Inferred LUE (gC/MJ^{-1} APAR) for boreal regions (1,2) for the base inversion (#1) and the scenario with alternate APAR (FASIR–NDVI) field (inversion #3). Inversion #1 is represented by filled circles for both basis regions, and inversion #3 is given by open diamonds for both basis regions.

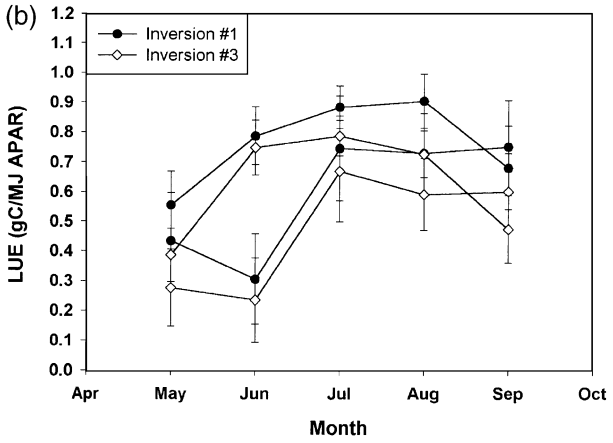

Fig. 2b (b) The average percent cover of deciduous vegetation for land regions north of 56°N. North America is represented by filled circles, Eurasia by open triangles. This figure is calculated using the fields of DeFries *et al*. (1999)

to match the CO_2 observations and slightly alters the inferred LUE seasonality. As a result, the growing-season mean boreal LUE asymmetry between North America and Eurasia is reduced slightly. The inferred LUE is also somewhat sensitive to the APAR field input. The FASIR–NDVI APAR values (inversion #3) are slightly higher than the NDVI APAR values (inversion #1) in these basis regions, producing lower inferred LUE values (Fig. 2b). The offset between growing-season mean LUE values for these boreal regions is preserved, as are the seasonality differences.

Differences in vegetation structure caused by the greater tree cover in Eurasia (DeFries *et al*., 1999) may also affect the fPAR–NDVI relationship (F. Huemmrich, personal communication), and thus the difference we infer between boreal North America and Eurasia. The higher Eurasian LUE values may result from a bias toward lower fPAR (Goward & Huemmrich, 1992; Huemmrich & Goward, 1997; Huemmrich, 2001). The distinct seasonal profiles of these two basis regions, however, suggest that this effect alone cannot explain the difference (Fig. 1).

The boreal LUE asymmetry is consistent with differences in ecosystem physiology and growth form between the regions. An outstanding distinction between Eurasia and North America north of 56°N is the much higher deciduous tree cover in Eurasia. While the average total tree cover is $\sim$40% higher in boreal Eurasia, the average deciduous tree cover is $\sim$300% higher in boreal Eurasia than boreal North America (DeFries *et al*., 1999) (Fig. 3). In Siberia, deciduous needleleaf Larch (*Larix*) forests dominate the landscape, covering nearly 280 million ha (Gower & Richards, 1990; Shvidenko & Nilsson, 1994; DeFries *et al*., 1999). The inferred LUE profiles for these boreal regions agree with expectations for deciduous or evergreen vegetation. The sharp spring increase and autumn decrease in LUE inferred for boreal Eurasia (region 2) would be expected for deciduous vegetation with relatively sharp leaf-on and leaf-off times (Waring *et al*., 1995; Bassow & Bazzaz, 1998; Morecroft & Roberts, 1999; Turner *et al*., 2003). By contrast, the LUE pattern inferred for boreal North America is consistent with the less sharply defined seasonality of evergreen coniferous vegetation (Hollinger *et al*., 1999; Turner *et al*., 2003). The delayed LUE increase in this region is consistent with the increase in leaf physiological activity and light-saturated photosynthesis accompanying spring warming in these ecosystems (Middleton *et al*., 1997; Lucht *et al*., 2002).

Empirical and theoretical evidence support a higher LUE for Larch forests than boreal evergreen conifer forests. A recent compilation of LUE observations for various ecosystem types (Gower *et al*., 1999) indicates a higher LUE for deciduous trees than evergreen trees, in both boreal and temperate forests. Other workers found a higher LUE for boreal aspen trees than sympatric black spruce trees (Goetz & Prince, 1998), a finding confirmed by more recent work using different methods (F. Huemmrich, personal communication). Another compilation (Ruimy *et al*., 1994) reported higher LUE values for conifers than deciduous trees, although it included temperate, boreal, and alpine forests in the coniferous classification, whereas the deciduous class includes only temperate forests, so a direct comparison is difficult. Taken together, these studies suggest a higher LUE for deciduous trees than evergreen trees, which would support the hypothesis of higher LUE in boreal Eurasian regions resulting from a greater deciduous tree fraction.

However, these LUE data are from deciduous broadleaved trees, and almost no data exist on the LUE of Larch species. The only published data suggest a much higher photosynthetic quantum yield and thus LUE for Siberian Larch trees relative to Canadian boreal conifers (Hollinger *et al*., 1998). These data are from an eddy flux study in east Siberia that calculated a quantum yield for a *Larix gmelinii* canopy in east Siberia of $\sim$0.01 $molCO_2\,mol^{-1}$ incident PAR, which corresponds to $\sim 0.55\,gC\,MJ^{-1}$ incident PAR. To estimate the quantum yield relative to absorbed rather than incident PAR, we used a simple Beer–Lambert formulation for fPAR (Ruimy *et al*., 1999) and the observed canopy leaf area index (Schulze *et al*., 1995) to calculate a quantum yield of $\sim 1.2\,gC\,MJ^{-1}$ APAR. We used a light extinction coefficient (k) of 0.5, which is typical for conifer forests (Ruimy *et al*., 1999). Varying this coefficient by plus or minus 60% produces quantum yield estimates of 2.45 and $0.89\,gC\,MJ^{-1}$ APAR.These estimates are larger than the reported quantum yield of a boreal evergreen conifer jack pine stand (0.66 gC/MJ APAR) and comparable to the quantum yield of a temperate mixed deciduous forest (0.83 gC/MJ APAR) (Baldocchi & Vogel, 1996).

Despite the sparsity of Larch LUE data, there are other ecophysiological data that support the hypothesis of a relatively high LUE for these trees. Two studies (Gower & Richards, 1990; Kloeppel *et al*., 1998) report much higher leaf nitrogen concentrations and greater specific leaf areas in Larch trees relative to co-occurring evergreen conifers, traits that are correlated with the higher photosynthetic potential typical of broadleaf deciduous species (Reich *et al*., 1997). Similarly, the midsummer nitrogen concentration of Larch needles in eastern Siberia (Schulze *et al*., 1995; Vygodskaya *et al*., 1997) was roughly twice that of the midsummer average N concentration of evergreen conifer needles measured in Canada (Middleton *et al*., 1997). The higher

N concentration in Siberian Larch needles is reflected in their relatively high rates of light-saturated maximum photosynthesis: $\sim 10\,\mu mol\,m^{-2}\,s^{-1}$ for *Larix gmelinii* in east Siberia (Vygodskaya *et al*., 1997) vs. a midsummer mean of $4.9\,\mu mol\,m^{-2}\,s^{-1}$ for jack pine and black spruce (Middleton *et al*., 1997). These comparisons suggest a higher LUE for Larch trees, as LUE is positively correlated with light-saturated photosynthetic rates, which are directly related to the N-rich Rubisco enzyme concentration in leaves (Monteith, 1977; Choudhury, 2001).

Additional correlative evidence for the enhanced LUE of Larch trees is the higher intercellular:ambient CO_2 ratio (Ci/Ca), ~ 0.7, for Larch trees relative to co-occurring evergreen conifers as estimated from carbon isotope data (Kloeppel *et al*., 1998) and as calculated using gas exchange measurements (Vygodskaya *et al*., 1997). The enhancement in intercellular CO_2 pressure for Larch trees relative to co-occurring conifers corresponds to $\sim 2.5\,Pa$, which is sufficient to increase the leaf-level quantum yield up to 5%. This would increase gross LUE, or GPP-LUE, especially under light-limited conditions. Although this is a small enhancement, C_i/C_a ratios and ^{13}C discrimination correlate well with other aspects of the deciduous leaf habit (Brooks *et al*., 1997) that seem to confer higher LUE relative to evergreen leaves. As Reich *et al*. (1997) demonstrated for a wide range of plant types, leaf photosynthetic rates increase with decreasing life span, leaf nitrogen concentration, and the ratio of leaf surface area to mass. All of these characteristics are typical of the deciduous leaf habit, and a higher photosynthetic rate would correspond to higher GPP-LUE.

Finally, Goetz and Prince (1998) present evidence that the higher LUE of boreal deciduous aspen trees relative to evergreen spruce trees is caused by differences in the proportion of carbon consumed by autotrophic respiration. The maintenance costs of year-round foliage and a greater amount of foliage biomass should decrease the LUE of evergreen conifers relative to deciduous trees. The absolute amount of foliage biomass in Larch canopies is smaller than comparable evergreen conifers (Schulze *et al*., 1995). The average percent of aboveground carbon contained in foliage of east Siberian Larch canopies is $\sim 3\%$ (Schulze *et al*., 1995), comparable to the percentage for boreal aspen stands ($\sim 1\%$) and much lower than that of boreal evergreen conifers ($\sim 12\%$) in North America (Gower *et al*., 1997).

Whether or not the higher Eurasian LUE results from the presence of Larch forests, the boreal asymmetry found here is consistent with a recent analysis (Schimel *et al*., 2001) that compared inverse model studies of net carbon storage for North America and Eurasia. The inverse model results were recast in more ecologically meaningful terms, specifically, the storage per unit ground area, per unit vegetated area, and normalized by the growing season length. In all cases, the values for Eurasia were consistently higher than North America by 10–20%. Another study, by Miller *et al*. (2003), used NOAA CMDL atmospheric CO_2 and $\delta^{13}C$ data to estimate intermediate-scale terrestrial discrimination against $^{13}CO_2$. Consistent with our findings and those of Schimel *et al*. (2001), they found higher discrimination values in Europe and Asia than in North America. These results agree with global modeling studies by Lloyd and Farquhar (1994) and Kaplan *et al*. (2002) that predict higher carbon isotope fractionation in Eurasia than in North America. Interestingly, these models also predict some of the highest terrestrial carbon isotope fractionation values for cold deciduous biomes like Larch forests. Finally, unpublished research examining LUE at smaller scales also supports our findings. In this work, tower-scale PAR and carbon flux data from needleleaf evergreen forests are combined with satellite-derived fPAR estimates to calculate monthly NPP LUE (W. Buermann, 'Merging FLUXNET and satellite data to derive independent estimates of LUE', unpublished results.). The calculated LUE is consistently higher in European forests than North American forests.

These hemispherical differences in LUE, carbon storage, and discrimination suggest underlying differences in ecosystem structure and function, such as the mismatch in deciduous vegetation cover between boreal Eurasia and boreal North America. The differences also likely reflect other underlying differences between these two boreal zones that affect ecosystem characteristics. As noted by Baldocchi *et al*. (2000), the Canadian and Siberian boreal zones differ in their climate (Siberia is generally colder and drier), permafrost cover (Siberia has much more continuous and discontinuous permafrost cover (Bonan & Shugart, 1989), and forest age structure (Siberia's forest is much younger as a result of more recent disturbances (Shvidenko & Nilsson, 1994; Kolchugina & Vinson, 1995).

Northern tropical region

The inferred LUE for all land between 0°N and 24°N (region 7) displays a distinct seasonal pattern and high growing-season average values of $\sim 0.6\,gC\,MJ^{-1}$ APAR, the only land region with LUE values close to those of boreal regions (Table 3 and Fig. 4). High LUE values might be expected due to the abundance of C_4 grasses in this region (Still *et al*., 2003) and the physiology of the C_4 photosynthetic pathway that produces a high LUE. C_4 plants are characterized by

high growth rates and typically are most abundant in semi-arid, hot ecosystems. In contrast to C_3 plants, C_4 plants concentrate CO_2 around the Rubisco enzyme, effectively eliminating photorespiration and maintaining high quantum yields at high temperatures. Also, C_4 photosynthesis does not saturate as quickly with respect to light as does C_3 photosynthesis, and maximum light-saturated photosynthesis rates in C_4 plants are considerably higher than in C_3 plants (Collatz *et al.*, 1992). These factors should increase the ratio of carbon uptake to absorbed light under a range of environmental conditions. This prediction is supported by empirical (Ruimy *et al.*, 1994; Gower *et al.*, 1999) and modeling (Choudhury 2001) analyses. For example, the average measured C_4 crop LUE is 30–40% higher than the average C_3 crop LUE (Ruimy *et al.*, 1994; Gower *et al*,. 1999).

The distinct seasonality of inferred LUE in this region is striking and consistent with seasonal patterns in the relative amounts of C_3 and C_4 photosynthesis (Fig. 4). The seasonal LUE inferred for this region also closely corresponds with the total cloud fraction seasonal profile (Rossow *et al.*, 1996) and associated changes in the diffuse fraction of radiation. The precipitation pattern closely follows the cloud fraction pattern in this region, but it does not drive the inferred LUE profile via its effects on HR. The inferred seasonal LUE pattern in region 7 is similar between inversion experiments with differing HR fields (inversion #1 vs. inversion #2 – Fig. 5). One of the HR fields (RP95 – inversion #2) is strongly sensitive to precipitation, and predicts a more seasonal HR flux. The other HR field (CASA – inversion #1) is less sensitive to precipitation, and predicts a flatter seasonal HR profile. Despite these different HR profiles, the inferred seasonal LUE profile is similar in both cases (Fig. 5), with a slightly higher flux-weighted, growing-season mean LUE value for inversion #2.

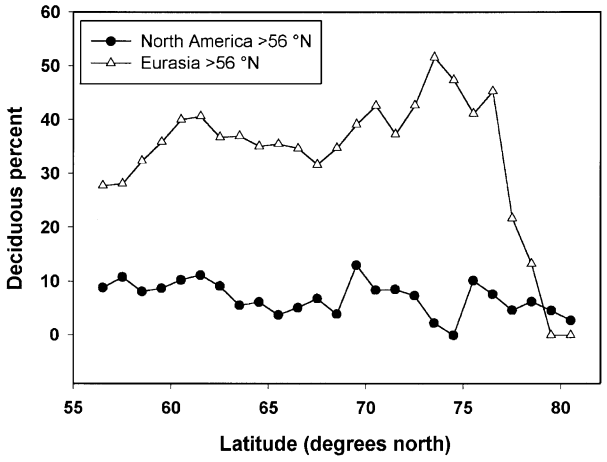

Fig. 3 Inferred growing season LUE (gC MJ^{-1} APAR) with SD for all land between 0°N and 24°N (open squares) averaged across the four inversion experiments. Also plotted are the average total cloud cover fraction (Rossow *et al.*, 1996) weighted by vegetated area (DeFries *et al.*, 1999) and the ratio of C_4 APAR to C_3 APAR (Still *et al.*, 2003) in open triangles and filled circles, respectively. The correlation coefficient between LUE and cloud cover fraction is 0.85, and the coefficient between LUE and C_4/C_3 APAR is 0.82.

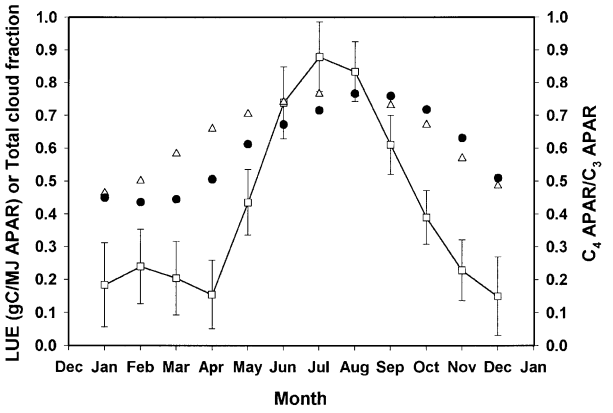

Fig. 4 Inferred growing season LUE (gC MJ^{-1} APAR) with SD for all land between 0°N and 24°N for inversion #1 (line and filled circles) and inversion #2 (line and open squares). Also plotted are the total heterotrophic respiration for this basis region predicted by the CASA model in filled circles (Van der Werf *et al.*, 2003) and the Raich & Potter (1995) model (open squares).

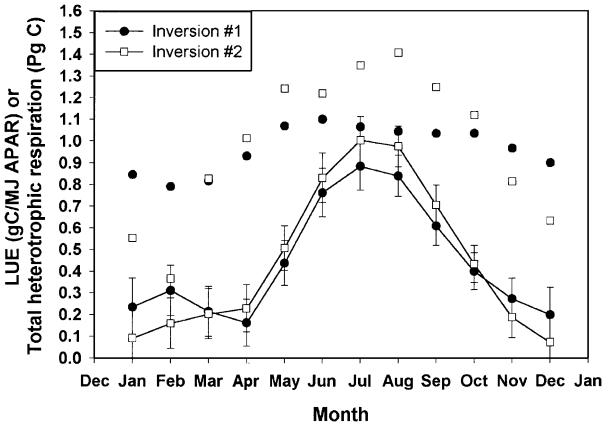

Fig. 5 Inferred growing season LUE (gC/MJ APAR) with standard deviation for all land between 0–24°N for inversion #1 (line and filled circles) and inversion #2 (line and open squares). Also plotted are the total heterotrophic respiration for this basis region predicted by the CASA model in filled circles (Van der Werf *et al.*, 2003) and the Raich and Potter (1995) model (open squares).

Despite the broad agreement between inferred LUE in this region and seasonal changes in vegetation physiology and cloud cover, it is unlikely that these latter effects entirely explain the LUE variations. The NDVI values may be artificially low in tropical regions due to persistent cloudiness. Also, the amplitude of seasonal LUE variation is too large to be driven only by increased C_4 vegetation activity and cloudiness. It is likely that seasonal drought impacts on soil water status would also strongly modify LUE in this region, and this phenomenon would be difficult to discern in our analysis. Finally, retrieval of tropical fluxes from atmospheric CO_2 observations is difficult, thanks to vigorous vertical mixing in these regions and a relative sparsity of low-latitude surface monitoring stations.

Conclusions

In this study, we combined inverse modeling in a framework with atmospheric CO_2 measurements, satellite observations, and an atmospheric transport model to infer large-scale physiological functioning of plants, specifically, the LUE of NPP. We deduce a consistent difference in LUE between boreal Eurasia and North America, a result of significance in the debate over partitioning the northern hemisphere carbon sink between these continents. This LUE difference may be caused, in part, by the much greater expanse of deciduous vegetation in Eurasia relative to North America as a result of the vast deciduous conifer (Larch) forests that dominate the landscape of central and east Siberia, covering some 280 million hectares. We also show that seasonal LUE variations in the northern tropics are strongly correlated with seasonal variations in C_4 vegetation production and cloud cover.

Large-scale relationships between inferred LUE and cloudiness support previous work at much smaller scales showing a relationship between LUE, cloudiness, and carbon uptake (Monteith, 1977; Hollinger *et al*., 1994, 1998; Gower *et al*., 1999; Freedman *et al*., 2001; Roderick *et al*., 2001; Gu *et al*., 2002). However, more research clearly needs to be conducted in order to decisively make such a connection between LUE and cloudiness at the scales of our inversion.

This study demonstrates an approach for bridging the scales between top-down estimates of regional scale carbon exchange and site-specific, bottom-up ecological observations. Besides LUE, other ecophysiological properties that characterize plants across an ecosystem are likely to be scale-invariant. These properties provide a multidimensional means for testing our understanding of ecosystem fluxes and carbon dynamics at multiple spatial scales.

Acknowledgements

Comments by D. Baldocchi, W. Riley, F. Huemmrich, D. Schimel, and anonymous reviewers improved the manuscript. The deciduous cover dataset was kindly provided by R. DeFries. We thank G. Van der Werf for providing the CASA HR fields and J. John for computing support. This research was supported by an appointment (CJS) to the Alexander Hollaender Distinguished Postdoctoral Fellowship Program, as well as NASA (NAG5-11200, NAG5-9514) and NSF (ATM-9987457; OPP-0097439) awards to IYF and JTR.

References

Andres RJ, Marland G, Fung I *et al*. (1996) A 1 × 1 distribution of carbon dioxide emissions from fossil fuel consumption and cement manufacture, 1950–1990. *Global Biogeochemical Cycles*, **10**, 419–429.

Baldocchi DD, Vogel CA (1996) Energy and CO_2 flux densities above and below a temperate broad-leaved forest and a boreal pine forest. *Tree Physiology*, **16**, 5–16.

Baldocchi DD, Kellliher FM, Black TA *et al*. (2000) Climate and vegetation controls on boreal zone energy exchange. *Global Change Biology*, **6** (Suppl. 1), 69–83.

Bassow SL, Bazzaz FA (1998) How environmental conditions affect canopy leaf-level photosynthesis in four deciduous tree species. *Ecology*, **79**, 2660–2675.

Bishop JK, Rossow WB (1991) Spatial and temporal variability of global surface solar irradiance. *Journal of Geophysical Research*, **96**, 16839–16858.

Bonan GB, Shugart HH (1989) Environmental factors and ecological processes in boreal forests. *Annual Review of Ecology and Systematics*, **20**, 1–28.

Bousquet P, Peylin P, Ciais P *et al*. (2000) Regional changes in carbon dioxide fluxes of land and ocean since 1980. *Science*, **290**, 1342–1346.

Brooks JR, Flanagan LB, Buchmann N *et al*. (1997) Carbon isotope composition of boreal plants: functional grouping of life forms. *Oecologia*, **110**, 301–311.

Choudhury BJ (2001) Modeling radiation- and carbon-use efficiencies of maize, sorghum, and rice. *Agricultural and Forest Meteorology*, **106**, 317–330.

Collatz GJ, Ribas-Carbo M, Berry JA (1992) Coupled photosynthesis-stomatal conductance model for leaves of C_4 plants. *Australian Journal of Plant Physiology*, **19**, 519–538.

Dargaville R, McGuire AD, Rayner P (2002) Estimates of large-scale fluxes in high latitudes from terrestrial biosphere models and an inversion of atmospheric CO_2 measurements. *Climatic Change*, **55**, 273–285.

DeFries RS, Townshend JRG, Hansen MC (1999) Continuous fields of vegetation characteristics at the global scale at 1 km resolution. *Journal of Geophysical Research*, **104**, 16911–16923.

Enting IG, Trudinger CM, Francey RJ (1995) A synthesis inversion of the concentration and $\delta^{13}C$ of atmospheric CO_2. *Tellus B*, **47**, 35–52.

Esbensen SK, Kushnir Y (1981) *THE heat budget of the global ocean: An atlas based on estimates from surface marine observations*. Climate Research Institute, Oregon State University, Corvallis, Oregon.

Fan S, Gloor M, Mahlman J *et al*. (1998) A large terrestrial carbon sink in North America implied by atmospheric and oceanic carbon dioxide data and models. *Science*, **282**, 442–446.

Field CB, Behrenfeld MJ, Randerson JT *et al*. (1998) Primary production of the biosphere: integrating terrestrial and oceanic components. *Science*, **281**, 237–240.

Freedman JM, Fitzjarrald DR, Moore KE *et al*. (2001) Boundary layer clouds and vegetation-atmosphere feedbacks. *Journal of Climate*, **14**, 180–197.

Fung I, John J, Lerner J *et al*. (1991) 3-dimensional model synthesis of the global methane cycle. *Journal of Geophysical-Research*, **96** (D7), 13 033–13 065.

GLOBALVIEW-CO_2: Cooperative Atmospheric Data Integration Project – Carbon Dioxide CD-ROM (2001). NOAA CMDL, Boulder, Colorado, 2001; also available at ftp://ftp.cmdl.noaa.gov/ccg/co2/GLOBALVIEW/.

Goetz SJ, Prince SD (1998) Variability in carbon exchange and light utilization among boreal forest stands: implications for remote sensing of net primary production. *Canadian Journal of Forestry Research*, **28**, 375–389.

Goward SN, Huemmrich KF (1992) Vegetation canopy PAR absorptance and the normalized difference vegetation index: an assessment using the SAIL model. *Remote Sensing of the Environment*, **39**, 119–140.

Gower ST, Richards JH (1990) Larches: deciduous conifers in an evergreen world. *BioScience*, **40**, 818–826.

Gower ST, Vogel JG, Norman JM *et al*. (1997) Carbon distribution and aboveground net primary production in aspen, jack pine, and black spruce stands in Saskatchewan and Manitoba, Canada. *Journal of Geophysical Research*, **102**, 29 029–29 041.

Gower ST, Kucharik C, Norman J (1999) Direct and indirect estimation of leaf area index, f(APAR), and net primary production of terrestrial ecosystems. *Remote Sensing of the Environment*, **70**, 29–51.

Gu L, Baldocchi DD, Verma SB *et al*. (2002) Superiority of diffuse radiation for terrestrial ecosystem productivity. *Journal of Geophysical Research*, **107**.

Gurney K, Law R, Rayner P *et al*. (2000) *TransCom 3 Experimental Protocol*. Paper No. 207, Department of Atmospheric Science, Colorado State University, USA.

Gurney KR, Law RM, Denning AS *et al*. (2002) Towards robust regional estimates of CO_2 sources and sinks using atmospheric transport models. *Nature*, **415**, 626–630.

Hanan NP, Burba G, Verma SB *et al*. (2002) Inversion of net ecosystem CO2 flux measurements for estimation of canopy PAR absorption. *Global Change Biology*, **8**, 563–574.

Hollinger DY, Kelliher FM, Byers JN *et al*. (1994) Carbon dioxide exchange between an undisturbed old-growth temperate forest and the atmosphere. *Ecology*, **75**, 134–150.

Hollinger DY, Kelliher FM, Schulze ED *et al*. (1998) Forest–atmosphere carbon dioxide exchange in eastern Siberia. *Agricultural and Forest Meteorology*, **90**, 291–306.

Hollinger DY, Goltz SM, Davidson EA *et al*. (1999) Seasonal patterns and environmental control of carbon dioxide and water vapour exchange in an ecotonal boreal forest. *Global Change Biology*, **5**, 891–902.

Huemmrich KF, Goward SN (1997) Vegetation canopy PAR absorptance and NDVI: an assessment for ten tree species with the SAIL model. *Remote Sensing of the Environment*, **61**, 254–269.

Huemmrich KF (2001) The GeoSail model: a simple addition to the SAIL model to describe discontinuous canopy reflectance. *Remote Sensing of the Environment*, **75**, 423–431.

Kaminski T, Knorr W, Rayner PJ *et al*. (2002) Assimilating atmospheric data into a terrestrial biosphere model: a case study of the seasonal cycle. *Global Biogeochemical Cycles*, **16** (4), 1066.

Kaplan JO, Prentice IC, Buchman N (2002) The stable carbon isotope composition of the terrestrial biosphere: modeling at scales from the leaf to the globe. *Global Biogeochemical Cycles*, **16**, 1060.

Kloeppel BD, Gower ST, Treichel IW *et al*. (1998) Foliar carbon isotope discrimination in *Larix* species and sympatric evergreen conifers: a global comparison. *Oecologia*, **114**, 153–159.

Knorr W, Heimann M (1995) Impact of drought stress and other factors on seasonal land biosphere CO_2 exchange studied through an atmospheric tracer transport model. *Tellus B*, **47**, 471–489.

Kolchugina TP, Vinson TS (1995) Role of Russian forests in the global carbon balance. *Ambio*, **24**, 258–264.

Lafont S, Kergoat L, Dedieu G (2002) Spatial and temporal variability of land CO_2 fluxes estimated with remote sensing and analysis data over western Eurasia. *Tellus*, **54B**, 820–833.

Lloyd J, Farquhar GD (1994) ^{13}C discrimination during CO_2 assimilation by the terrestrial biosphere. *Oecologia*, **99**, 201–215.

Los SO, Justice CO, Tucker CJ (1994) A global 1 by 1 NDVI dataset for climate studies derived from the GIMMS continental NDVI. *International Journal of Remote Sensing*, **15**, 3493–3518.

Los SO, Collatz GJ, Sellers PJ *et al*. (2000) A global 9-yr biophysical land surface dataset from NOAA AVHRR data. *Journal of Hydrometeorology*, **1**, 183–199.

Lucht W, Prentice IC, Myneni RB *et al*. (2002) Climatic control of the high-latitude vegetation greening trend and Pinatubo effect. *Science*, **296**, 1687–1689.

Middleton EM, Sullivan JH, Bovard BD *et al*. (1997) Seasonal variability in foliar characteristics and physiology for boreal forest species at the five Saskatchewan tower sites during the 1994 Boreal Ecosystem–Atmosphere study. *Journal of Geophysical Research*, **102**, 28 831–28 844.

Miller JB, Tans PP, White JWC *et al*. (2003) The atmospheric signal of terrestrial carbon isotopic discrimination and its implication for partitioning carbon fluxes. *Tellus Series B*, **55**, 197–206.

Monteith JL (1977) Climate and the efficiency of crop production in Britain. *philosophical Transactions of the Royal Society of London. B*, **281**, 277–294.

Morecroft MD, Roberts JM (1999) Photosynthesis and stomatal conductance of mature canopy Oak (*Quercus robur*) and Sycamore (*Acer pseudoplatanus*) trees throughout the growing season. *Functional Ecology*, **13**, 332–342.

Nichol CJ, Lloyd J, Shibistova O *et al*. (2002) Remote sensing of photosynthetic-light-use efficiency of a Siberian boreal forest. *Tellus*, **54B**, 677–687.

Pacala SW, Hurtt GC, Baker D *et al*. (2001) Consistent land- and atmosphere-based U.S. carbon sink estimates. *Science*, **292**, 2316–2320.

Peylin P, Bousquet P, Ciais P *et al*. (2000) Differences of CO_2 flux estimates based on a 'time-independent' vs. a 'time-dependent' inversion method. In: *Inverse Methods in Global Biogeochemical Cycles* (eds Kasibhatla P, Heimann M, Rayner P, Mahowald N, Prinn RG, Hartley DE), pp. 295–309. American Geophysical Union, Washington, DC.

Potter CS, Randerson JT, Field CB *et al*. (1993) Terrestrial ecosystem production: a process-based model based on global satellite and surface data. *Global Biogeochemical Cycles*, **7**, 811–841.

Raich JW, Potter CS (1995) Global patterns of carbon dioxide emissions from soils. *Global Biogeochemical Cycles*, **9**, 23–36.

Raich JW, Potter CS, Bhagawati D (2002) Interannual variability in global soil respiration, 1980–94. *Global Change Biology*, **8**, 800–812.

Randerson JT, Thompson MV, Conway TJ *et al*. (1997) The contribution of terrestrial sources and sinks to trends in the seasonal cycle of atmospheric carbon dioxide. *Global Biogeochemical Cycles*, **11**, 535–560.

Randerson JT, Still CJ, Ballé JJ *et al*. (2002) The ^{13}C discrimination of arctic and boreal biome net CO_2 exchange inferred from remote atmospheric measurements and biosphere–atmosphere models. *Global Biogeochemical Cycles*, **16**, 1028.

Rayner PJ, Enting IG, Francey RJ *et al*. (1999) Reconstructing the recent carbon cycle from atmospheric CO_2, $\delta^{13}C$ and O_2/N_2 observations. *Tellus B*, **51**, 213–232.

Rayner PJ (2001) Constraining the global carbon budget from global to regional scales – the measurement challenge. In: *Global Biogeochemical Cycles in the Climate System* (eds Schulze ED, Heimann M, Harrison S, Holland E, Lloyd J, Prentice C, Schimel D), pp. 285–294. Academic Press, San Diego.

Reich PB, Walters MB, Ellsworth DS (1997) From tropics to tundra: global convergence in plant functioning. *Proceedings of the National Academy of Sciences USA*, **94**, 13730–13734.

Roderick ML, Farquhar GD, Berry SL (2001) On the direct effect of clouds and atmospheric particles on the productivity and structure of vegetation. *Oecologia*, **129**, 21–30.

Rossow WB, Walker AW, Beuschel DE *et al*. (1996) International Satellite Cloud Climatology Project (ISCCP) Documentation of New Cloud Datasets. WMO/TD-No. 737, World Meteorological Organization, 115pp.

Ruimy A, Saugier B, Dedieu G (1994) Methodology for the estimation of terrestrial net primary production from remotely sensed data. *Journal of Geophysical Research*, **99**, 5263–5283.

Ruimy A, Kergoat L, Bondeau A (1999) Comparing global models of terrestrial net primary productivity (NPP): Analysis of differences in light absorption and light-use efficiency. *Global Change Biology*, **5**, 56–64.

Running SW, Hunt ER (1993) In: *Scaling Physiological Processes Leaf to Globe* (eds Ehleringer JR, Field CB), pp. 141–158. Academic Press, San Diego.

Schimel DS, House JI, Hibbard KA *et al*. (2001) Recent patterns and mechanisms of carbon exchange by terrestrial ecosystems. *Nature*, **414**, 169–172.

Schulze ED, Schulze W, Kelliher FM *et al*. (1995) Aboveground biomass and nitrogen nutrition in a chronosequence of pristine Dahurian *Larix* stands in eastern Siberia. *Canadian Journal of Forest Research*, **25**, 943–960.

Sellers PJ, Tucker CJ, Justice CO *et al*. (1996) A revised land surface parameterization (SiB2) for atmospheric GCMs. Part II: The generation of global fields of terrestrial biophysical parameters from satellite data. *Journal of Climate*, **9**, 706–737.

Shvidenko A, Nilsson S (1994) What do we know about the Siberian forests? *Ambio*, **23**, 396–404.

Still CJ, Berry JA, Collatz GJ *et al*. (2003) The global distribution of C_3 and C_4 vegetation: carbon cycle implications. *Global Biogeochemical Cycles*, **17** (1), 1006.

Takahashi T, Feely RA, Weiss RF *et al*. (1997) Global air–sea flux of CO_2: an estimate based on measurements of sea–air pCO(2) difference. *Proceedings of the National Academy of Sciences USA*, **94**, 8292–8299.

Tans P, Fung I, Takahashi T (1990) Observational constraints on the global atmospheric CO_2 budget. *Science*, **247**, 1431–1438.

Trumbore SE, Gaudinski JB, Hanson PJ *et al*. (2002) Quantifying ecosystem-atmosphere carbon exchange with a ^{14}C label. *EOS, Transactions, AGU*, **83**, 265–268.

Turner DP, Urbanski S, Bremer D *et al*. (2003) A cross-biome comparison of daily light use efficiency for gross primary production. *Global Change Biology*, **9**, 383–395.

Van der Werf GR, Randerson JT, Collatz GJ *et al*. (2003) Carbon emissions from fires in tropical and subtropical ecosystems. *Global Change Biology*, **9**, 547–562.

Vygodskaya NN, Milyukova I, Varlagin A *et al*. (1997) Leaf conductance and CO_2 assimilation of *Larix gmelinii* growing in an eastern Siberian boreal forest. *Tree Physiology*, **17**, 607–615.

Wanninkhof R (1992) Relationship between wind-speed and gas-exchange over the ocean. *Journal of Geophysical Research*, **97**, 7373–7382.

Waring RH, Law BE, Goulden ML (1995) Scaling gross ecosystem production at Harvard Forest with remote sensing: a comparison of estimates from a constrained quantum-use efficiency model and eddy correlation. *Plant, Cell and Environment*, **18**, 1201–1213.